analytical chemistry

Article

Cite This: Anal. Chem. 2019, 91, 4092−4099

pubs.acs.org/ac

Measuring the Integrity of Gas-Phase Conformers of Sodiated 25-Hydroxyvitamin D3 by Drift Tube, Traveling Wave, Trapped, and High-Field Asymmetric Ion Mobility

Nicholas R. Oranzi,[†] Robin H. J. Kemperman,[†] Michael S. Wei,[†] Violeta I. Petkovska,[‡] Scott W. Granato,[‡] Benjamin Rochon,[‡] Julia Kaszycki,[§] Aurelio La Rotta,[§] Kevin Jeanne Dit Fouque,[∥,⊥] Francisco Fernandez-Lima,[∥,⊥] and Richard A. Yost*[,†]

[†]Department of Chemistry, University of Florida, Gainesville, Florida, United States

[‡]Axalta Coating Systems, Philadelphia, Pennsylvania, United States

[§]Excellims Corporation, Acton, Massachusetts, United States

[∥]Department of Chemistry and Biochemistry, Florida International University, Miami, Florida, United States

[⊥]Biomolecular Science Institute, Florida International University, Miami, Florida, United States

Supporting Information

ABSTRACT: Quantitation of the serum concentration of 25-hydroxyvitamin D is a high-demand assay that suffers from long chromatography time to separate 25-hydroxyvitamin D from its inactive epimer; however, ion mobility spectrometry can distinguish the epimer pair in under 30 ms due to the presence of a unique extended or "open" gas-phase sodiated conformer, not shared with the epimer, reducing the need for chromatographic separation. Five ion mobility mass spectrometers utilizing commercially available IMS technologies, including drift tube, traveling wave, trapped, and high-field asymmetric ion mobility spectrometry, are evaluated for their ability to resolve the unique open conformer. Additionally, settings for each instrument are evaluated to understand their influence on ion heating, which can drive the open conformer into a compact or "closed" conformer shared with the epimer. The four low-field instruments successfully resolved the open conformer from the closed conformer at baseline or near-baseline resolution at typical operating parameters. High-field asymmetric ion mobility was unable to resolve a unique peak but detected two peaks for the epimer, in contrast to the low-field methods that detected one conformer. This study seeks to expand the instrument space by highlighting the potential of each platform for the separation of 25-hydroxyvitamin D epimers.

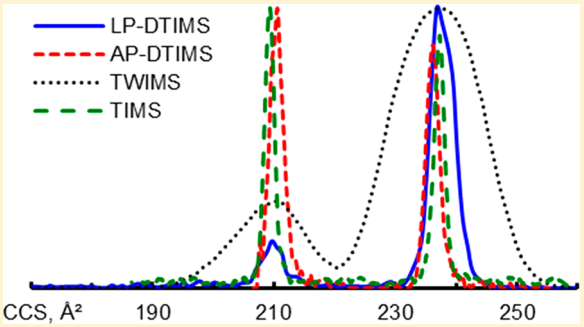

INTRODUCTION

The downstream metabolite of vitamin D, 25-hydroxyvitamin D (25OHD), is most noted for its role in regulating calcium absorption, gene transcription, cell signaling, and bone growth.[1] In response to increasing evidence linking vitamin D deficiency to diabetes, cardiovascular disease, and other chronic conditions,[2] the demand for testing of the serum concentration has risen.[3] Vitamin D, produced upon exposure to UV radiation or consumed from dietary sources, is readily converted to 25OHD in the liver, which binds to the vitamin D binding protein as the main circulating metabolite.[4] By itself 25OHD is inactive, but it is further metabolized in the kidneys to form 1,25-dihydroxyvitamin D ($1,25(OH)_2D$), the active calcium-regulating metabolite, or 24,25-dihydroxyvitamin D ($24,25(OH)_2D$), to be excreted as waste.[1] Although measurement of $1,25(OH)_2D$ is used to identify calcium metabolism disorders, it is of little value in assessing overall vitamin D health.[5] Instead, the ratio of 25OHD to $24,25(OH)_2D$[6] or the measurement of unbound 25OHD has been proposed as a better marker for vitamin D sufficiency;[7] nevertheless, because of its much higher circulating concentration and long half-life, total (bound and unbound) 25OHD remains the most common target of analytical assays.[8]

Liquid chromatography−tandem mass spectrometry (LC-MS/MS) is considered the preferred mode of analysis for vitamin D quantitation due to its chemical specificity and sensitivity;[9] however, a major bottleneck during LC-MS/MS analysis is the lengthy chromatography time required to separate 25OHD from its naturally occurring stereoisomer, 3-epi-25-hydroxyvitamin D (epi25OHD).[10] Structures for 25OHD3 and epi25OHD3 are provided in the Supporting Information. This metabolite is formed endogenously; however, its biological role is currently unknown.[11] Serum concentrations in adult populations are typically low, below

Received: December 13, 2018
Accepted: February 20, 2019
Published: February 26, 2019

DOI: 10.1021/acs.analchem.8b05723
Anal. Chem. 2019, 91, 4092−4099

5%, but can exceed 50% of total 25OHD in infants.[8] Failure to resolve the epimer can lead to overestimation of the 25OHD concentration[12,13] and can lead to a missed diagnosis of vitamin D deficiency.[10,14] Despite the potential for misdiagnosis, to increase sample throughput the epimer is often not quantified.[15]

Recent work from our laboratory has demonstrated the rapid separation of 25OHD and epi25OHD using ion mobility spectrometry (IMS) coupled with liquid chromatography and mass spectrometry (LC-IM-MS).[16] Ion mobility mass spectrometry is a gas-phase separation technique that resolves ions on the basis of differences in their mass, charge, and collision cross section (CCS).[17] In the simplest iteration, drift-tube ion mobility spectrometry (DTIMS),[17,18] ions travel under the influence of a uniform electric field in the presence of a neutral buffer gas, commonly nitrogen. Larger ions undergo more frequent collisions with the buffer gas and are detected at a later drift time relative to smaller ions;[19] ions can be described by their gas-phase mobility, K, which is a ratio of an ion's velocity to the strength of the electric field.[20] Utilizing this principle, further implementations of IMS have been developed, including traveling wave ion mobility spectrometry (TWIMS),[21] where the ions are propelled by an electric potential wave through an rf-confining drift tube, or trapped ion mobility spectrometry (TIMS),[22] where ions driven by a gas pressure gradient are trapped in space by an opposing electric field gradient. High-field asymmetric waveform ion mobility spectrometry (FAIMS)[23] uses a high voltage to induce a nonlinear change in mobility between low and high fields as a separation means. Detailed descriptions of each implementation are given in the respective references.

Despite the commercial availability of IMS instruments, adoption of IMS for small-molecule quantitation has been slow partially due to the initial investment costs, uncertainty of moving from the traditional LC/MS/MS-based methods that dominate routine quantitation, and lack of high-demand applications to justify the investment in new instrumentation. Robust, instrument-independent, and analytically relevant methods will drive adoption of IMS in high-throughput clinical, environmental, and forensic laboratories. Rapid quantitation of 25OHD in human serum using LC/IM-MS is one such example of a high-demand assay that benefits from IMS by reducing chromatography time and improving sample throughput.

To date, quantitation of 25OHD using LC/IM-MS has only been performed on a low-pressure DTIMS instrument (LP-DTIMS).[16,24] Chouinard et al. found that two mobility peaks are detected using LP-DTIMS for the sodiated adduct of 25OHD. Modeling identified each of these conformers as a compact (closed) conformer, where both hydroxyl groups interact with the sodium ion, and an extended (open) conformer, where one hydroxyl group interacts with the sodium ion, while only the closed conformer is detected for epi25OHD[24] (3D models of each conformer can be found in the cited work). Because the open conformer is unique to 25OHD, it can be individually monitored to quantify 25OHD without interference from the epimer, reducing sample analysis time since chromatographic resolution of the epimers is not needed. The ratio of the open to closed conformer has been shown to be sensitive to rf heating induced by the ion optics of the mass spectrometer, specifically within the ion accumulation trap prior to injection into the drift tube, where the kinetically trapped open conformer can convert to the closed conformer. Conversion of the open conformer can lead to reduced signal to noise or bias during quantitation. With careful control of instrument settings and use of an isotopically labeled internal standard, bias associated with conversion from open to closed conformers can be avoided during LC-IM-MS quantitation.[16] The suitability of an IMS technology for use in a quantitative assay is predicated on its ability to resolve the two conformers and preserve the unique open conformer to avoid introducing bias. Therefore, the separation of sodiated 25OHD conformers using IMS implementations in addition to LP-DTIMS, including atmospheric pressure DTIMS (AP-DTIMS), TWIMS, TIMS, and FAIMS, is the focus of this work.

Internal energy deposition during IMS separations is of critical interest in considering which ion mobility technology is to be used. Thermometer ions, ions with known fragmentation pathways and well-characterized dissociation energies, can model changes to ion internal energy;[25] however, many thermometer ions, such as benzylpyridinium ions, are not commercially available, and those that are, such as leucine enkephalin, require high activation energies and multiple pathways for dissociation.

The work within this study establishes a relationship between internal energy and conversion of open to closed conformers of sodiated 25OHD using benzylpyridinium thermometer ions to measure internal energy changes during the IMS separation and shows that, in addition to its clinical relevance, sodiated 25OHD can be an effective thermometer ion for probing IMS processes. Five commercially available IMS instruments are evaluated for their ability to resolve the sodiated 25OHD conformers, with the four low-field instruments resolving the conformers at baseline or near-baseline resolution. Using sodiated 25OHD as a thermometer ion, instrumental factors affecting the conformer ratios, related to internal energy changes, are explored for each platform. Rather than benchmark each instrument, this study demonstrates that separation of 25OHD epimers is not limited to a single platform but is possible on a broad class of ion mobility instruments.

MATERIALS AND METHODS

Chemicals. Ethanol solutions of 25-hydroxyvitamin D3-[$^2H_6$] and 3-epi-25-hydroxyvitamin D3 were purchased from Isosciences (Ambler, PA). Material purity was validated by the manufacturer by ^{1}H NMR and HPLC. The use of the isotopically labeled version allows for mass discrimination when both vitamin D metabolites are coinfused. It has been demonstrated previously that the labeled and unlabeled compounds behave identically.[16] *p*-(Trifluoromethyl)benzyl chloride, *p*-chlorobenzyl chloride, *p*-methylbenzyl chloride, and pyridine were purchased from MilliporeSigma (St. Louis, MO), and methanol (LC/MS grade) was purchased from Fisher Scientific (Pittsburgh, PA). Working solutions consisted of 5 μg/mL of 25-hydroxyvitamin D3-[$^2H_6$] (d_6-25OHD3) and epi25OHD3, which were distributed to separate laboratories for analysis. Because sensitivity was not a goal of the study, no guidance was given on final test concentration to allow flexibility for differences in ion transmission. For traveling wave experiments, the CCS calibration solution consisted of 50 μg/mL of DL-polyalanine in methanol (MilliporeSigma), and for DTIMS and TIMS experiments, an ESI tune mix was used (Agilent, Santa Clara, CA). Drift times for the sodiated adducts of d_6-25OHD3 (m/z 429.3600) and epi25OHD3 (m/z 423.3239) were extracted and the peak

DOI: 10.1021/acs.analchem.8b05723
Anal. Chem. 2019, 91, 4092−4099

areas integrated using the instruments' respective vendor software. The percentage of open conformer is calculated as

$$\text{percent open conformer} = \frac{A_{\text{open}}}{A_{\text{open}} + A_{\text{closed}}} \times 100 \quad (1)$$

where A_{open} and A_{closed} are the integrated peak areas of the open and closed conformers, respectively.

Para-substituted benzylpyridinium (BP) salts were prepared by combining the substituted benzyl chloride with excess pyridine and heating to 60 °C for 3 h. Excess pyridine was evaporated, and the remaining BP salts were used without further purification.[26]

Instrumentation. Detailed descriptions of instrument settings and experimental conditions are given in the Supporting Information. Briefly, low-pressure drift tube experiments were performed on an Agilent 6560 ion mobility quadrupole time of flight (Q-ToF) mass spectrometer (Santa Clara, CA). Atmospheric-pressure drift-tube experiments were performed on an Excellims MA3100 instrument (Acton, MA) coupled to a Thermo Scientific Orbitrap Focus mass spectrometer (Bremen, Germany). Traveling wave experiments were performed on a Waters SYNAPT G1 Q-ToF mass spectrometer (Milford, MA). Trapped ion mobility experiments were performed on a custom-built nanoESI-TIMS coupled to an Impact Q-ToF mass spectrometer (Bruker Daltonics Inc., Billerica, MA). High-field asymmetric IMS experiments were performed using the Owlstone ultraFAIMS-T1 instrument (Cambridge, U.K.) coupled to a Thermo LTQ linear ion trap mass spectrometer (Waltham, MA). For each instrument, conditions were optimized to maximize resolving power and peak to peak resolution.

RESULTS AND DISCUSSION

Internal Energy-Driven Interconversion. Benzylpyridinium (BP) ions are used widely in mass spectrometry for assessing changes to the internal energy (IE) distribution of ion populations in response to mass spectrometry processes.[25,27−30] These ions are attractive due to the simple fragmentation pathway (loss of neutral pyridine) and variety of substitutions with unique critical energies for dissociation to model changes to the IE distribution.[25] The structures and fragmentation scheme of the para-substituted BP ions used in this work are provided in the Supporting Information. The survival yield of the thermometer ions refers to the proportion of the parent ion that survives to be detected so that a decrease in survival yield is representative of an increase in fragmentation and, in turn, increase in the IE distribution. Survival yield is calculated as

$$\text{survival yield} = \frac{I_{\text{parent}}}{I_{\text{parent}} + I_{\text{fragment}}} \times 100 \quad (2)$$

where I_{parent} and I_{fragment} are the peak intensities of the parent and fragment, respectively. For each set of instrument conditions, the survival yield for each parent ion is calculated, plotted against the critical energy required for fragmentation (E_0),[26] and fitted to a sigmoid bounded by 100% and 0% representing no dissociation at high E_0 and complete dissociation at low E_0. The first derivative of this sigmoidal breakdown curve represents the internal energy distribution of the BP ions. Although useful for a qualitative description of internal energy in response to instrument settings, the results should not be interpreted quantitatively, since this method does not account for a kinetic shift (the energy required to drive dissociation on the experimental time scale) or for the IE distribution of sodiated d_6-25OHD3 being much different from that of the BP ions due to the greater number of degrees of freedom and significant differences in structure.[25]

Although previous work demonstrated that rf heating was driving conversion of the open conformers to the closed conformer, a definitive link with internal energy was not established. Additionally, the magnitude of the energy deposition, relative to established methods, was not investigated. Using BP thermometer ions, the relative sensitivity of the conformer conversion is more clearly defined, and the conversion of 25OHD3 conformers can be used to probe internal energy deposition on other IMS instruments and identify which parameters must be considered to minimize ion heating and preserve the open conformer. Survival yields of para-substituted BP ions, infused on the LP-DTIMS, are plotted with percent of open sodiated d_6-25OHD3 conformers with respect to exit grid 1 low potential in Figure 1, which

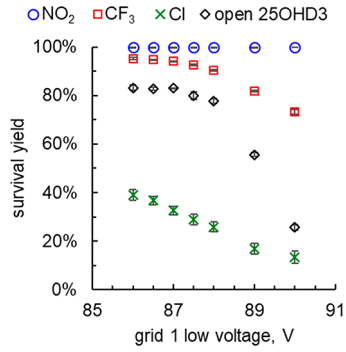

Figure 1. Survival yield of para-substituted benzylpyridinium ions and percent open conformer of sodiated d_6-25OHD3 in response to trapping voltages within the ion accumulation region of the LP-DTIMS instrument. The percent of open conformer decreases more rapidly than the survival yield of the thermometer ions, suggesting that sodiated d_6-25OHD3 is more sensitive to internal energy changes.

defines the potential of the first trapping grid at the exit of the accumulation trap. Previous work has shown radial dispersion of the ions at high grid voltages resulting in a decrease in the percent of open conformer[16] and in these experiments is accompanied by a decrease in the survival yield of the BP ions. Figure S1 shows the IE distribution derived from the derivative of the breakdown curves at low, moderate, and high grid 1 low voltage. As the grid voltage increases, the IE distribution shifts to higher average energy with a wider distribution. At higher grid voltages, the percentage of open conformer decreases, using BP ions to measure IE, providing unambiguous evidence that changes in conformer ratios from open to closed arise from an increase in average IE. Between low and high grid voltages, the survival yield of *p*-chlorobenzylpyridinium, which has the lowest critical dissociation energy of the three ions, decreases from 40% to 15% while sodiated d_6-25OHD3 changes substantially from 84% to 22% of open conformers. Less energy is required to convert the fragile open conformer to closed than to fragment the BP thermometer ions. Leucine enkephalin, a thermometer ion often used to characterize IE,[29,31−33] is structurally more similar to 25OHD3, containing a similar number of degrees of freedom, and therefore has a

DOI: 10.1021/acs.analchem.8b05723
Anal. Chem. 2019, 91, 4092−4099

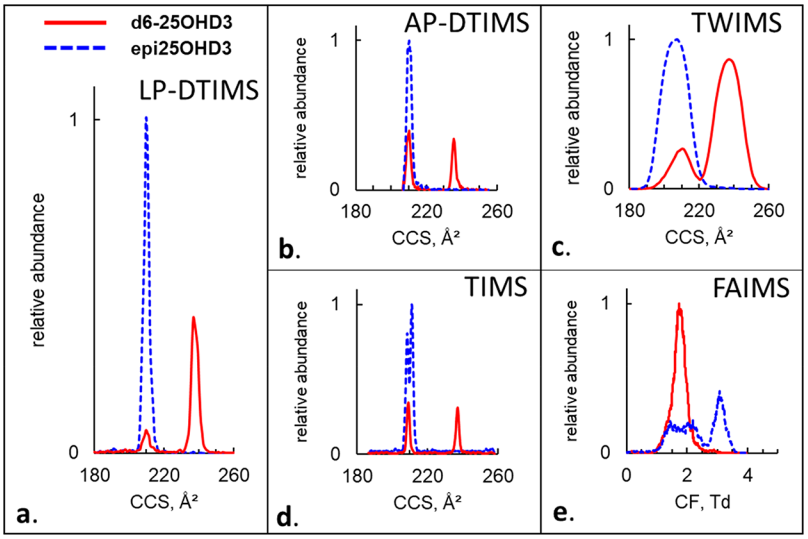

Figure 2. Collision cross section and dispersion field spectra of sodiated d_6-25OHD3 (429.3600) and epi25OHD3 (m/z 423.3239) for five commercial IMS implementations: (a) low-pressure drift tube ion mobility spectrometry (LP-DTIMS); (b) atmospheric-pressure drift tube ion mobility spectrometry (AP-DTIMS); (c) traveling wave ion mobility spectrometry (TWIMS); (d) trapped ion mobility spectrometry (TIMS); (e) high-field asymmetric waveform ion mobility spectrometry (FAIMS).

Table 1. Collision Cross Sections (CCS) for Low-Field Ion Mobility Methods in Comparison to Stepped-Field Drift Tube Ion Mobility Measurements[a]

	epi25OHD3		d_6-25OHD3 closed		d_6-25OHD3 open	
	CCS, Å^2	ΔCCS, %	CCS, Å^2	ΔCCS, %	CCS, Å^2	ΔCCS, %
ref	209.0		209.9		236.6	
LP-DTIMS	209.6	0.29	209.6	−0.14	236.7	0.04
AP-DTIMS	210.6	0.76	210.2	0.14	236.3	−0.13
TWIMS	207	−0.97	209	0.48	238	0.42
TIMS	208.6/211.2	−0.43/1.0	209.2	−0.33	237.1	−0.21

[a]Two peaks are observed by TIMS for sodiated epi25OHD3. Reference values were obtained from stepped-field measurements on the LP-DTIMS instrument.

potentially more analogous IE distribution. However, when it is infused to measure ion heating, during trapping grid voltage experiments the abundance of fragment ions is too low to accurately measure survival yield. In comparison to traditional thermometer ions such as the BP ions and leucine enkephalin, sodiated d_6-25OHD3 appears to be more sensitive to IE changes and, in contrast to protein ions such as cytochrome c with many intermediate conformations,[34] has only two possible conformers, simplifying spectral interpretation. In this study, d_6-25OHD3 is utilized with two goals: to determine which IMS platforms can separate the sodiated d_6-25OHD3 conformers and to determine sources of ion heating using sodiated d_6-25OHD3 as a thermometer ion.

25-Hydroxyvitamin D3 across IMS Platforms. Understanding the separation of vitamin D metabolites across IMS technologies is the goal of this work; the comparison among platforms is of value to laboratories interested in adapting the previously published LC/IM-MS quantitation method and ion mobility spectrometrists concerned with internal energy deposition during IMS analysis. The relative advantages and disadvantages of each ion mobility platform is discussed by D'Atri et al. among others.[35] As shown in Figure 2, all four low-field IMS methods (LP-DTIMS, AP-DTIMS, TWIMS, and TIMS) resolve the two sodiated d_6-25OHD3 conformers. Both DTIMS and TWIMS resolve a single sodiated epi25OHD3 conformer, and TIMS partially resolves a second peak for sodiated epi25OHD3, while FAIMS resolves only one sodiated d_6-25OHD3 peak but two sodiated epi25OHD3 peaks. A compilation of the CCS and CF spectra of sodiated d_6-25OHD3 and epi25OHD3 (m/z 429.3611 and 423.3239, respectively) from the five IMS platforms is presented in Figure 2, and a summary of the CCS and bias of low-field IMS platforms is presented in Table 1. For each method, the stepped-field CCS values obtained by the LP-DTIMS instrument are considered the reference values (Table 1), since sodiated d_6-25OHD3 is well-characterized[16,24] and the ability to make direct and accurate CCS measurements without external calibrants using the stepped-field method is well documented.[18,36] A description of the stepped-field method is given in the Supporting Information. Bias is calculated as the relative percent difference between the measured CCS and the stepped-field CCS measurement. Good agreement is found between single and stepped field CCS measurements on the LP-DTIMS instrument. Stow et al. compared single and stepped field CCS measurements and reported an average bias under 0.5%, but 25OHD3 is not among the compounds included in that study.[36] Table S2 contains calculated resolving power (R_p), a measure of peak width, and open to closed peak resolution (R_s), a measure of peak separation, where baseline resolution is defined as $R_s > 1.5$; equations for calculating R_s and R_p are given in the Supporting Information. The average resolving power of 51 by LP-DTIMS is consistent with values

DOI: 10.1021/acs.analchem.8b05723
Anal. Chem. 2019, 91, 4092−4099

expected for compounds using this instrument[18] and is sufficient to achieve baseline resolution, where R_s = 3.3, and the signal from the closed conformer will not interfere with that of the open conformer. In this work, source-related effects on the initial conformer distribution were not explicitly investigated. As ionization conditions can influence the initial IE, it is reasonable to assume some differences in the initial ratio of open and closed conformers for each system; however, this could differ on a single instrument on the basis of which specific source type is used. Regardless of the source used, sources of ion heating can be measured for each instrument by monitoring changes to the initial distribution.

Atmospheric-Pressure Drift Tube IMS. Both open and closed conformers of the sodiated d_6-25OHD3 are resolved by the AP-DTIMS instrument. Calculated CCS values of 210.2 Å^2 for the earlier drift peak and 236.3 Å^2 for the later drift peak are measured with an average bias of 0.25% relative to the reference values (Table 1). The single epimer peak coelutes with the earlier conformer of sodiated d_6-25OHD3, and the low bias between measured and reference CCS values gives high confidence that the observed conformers match the conformers detected by the LP-DTIMS instrument. Under typical operating conditions with a drift gas temperature of 180 °C, the value for percent open conformers is 56%, substantially different from that at low pressure where 86% open conformers is measured. R_p is much higher, 81 versus 51, as is R_s = 6.1 versus R_s = 3.3 for low pressure. Fundamental differences between the instruments operating in different pressure regimes must be considered to understand the observed differences.

At atmospheric pressure, ions are directly gated into the drift region with much higher gas temperatures to achieve complete desolvation, but the higher temperatures can be problematic for thermally labile ions; therefore, the effects of gas temperature must be evaluated to understand the sensitivity of sodiated d_6-25OHD3 to thermally induced interconversion. The percent of open conformer is measured with gas temperatures between 80 and 250 °C in Figure 3. Because

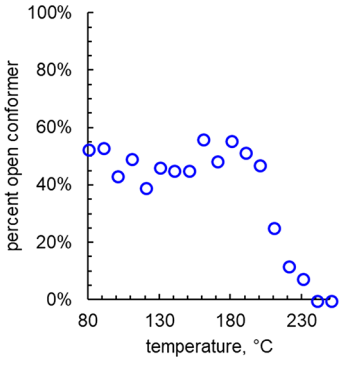

Figure 3. Percent open conformer of sodiated d_6-25OHD3 with respect to the desolvation gas temperature in the AP-DTIMS instrument. The conformer ratio is stable until 200 °C. Above 200 °C the open conformer converts into the closed conformer.

of the short distance of the drift tube, it is assumed that the gas temperature is consistent across the length of the drift tube. Between 80 and 200 °C, the percentage of open conformer remains constant, beginning to decrease as temperatures climb above 200 °C (fluctuation can be attributed to low signal intensity at low temperatures from incomplete desolvation).

This instrument features dc-only ion guides and thus sodiated d_6-25OHD3 cannot undergo rf heating; more likely, thermal heating from the desolvation gas drives interconversion. Despite the lower ratio of open conformers observed by AP-DTIMS, the ratio remains constant across a wide range of temperatures, and interconversion is a minor concern during LC-IM-MS method development if the desolvation temperature remains below 200 °C. At the same time, the temperature must be high enough to completely desolvate the ions to maximize transmission.

Traveling Wave IMS. Using traveling wave IMS, two distinct conformers are detected for sodiated d_6-25OHD3 at 209 Å^2 and 238 Å^2, whereas only one conformer is detected for sodiated epi25OHD3 at 207 Å^2 (Figure 2c). The number and relative CCS of each conformer match those of DTIMS experiments; thus, the early conformers (209 Å^2 and 207 Å^2) likely correspond to the closed conformer and the later conformer (238 Å^2) corresponds to the open conformer. The assignments of the conformers are confirmed by CCS measurements (Table 1), where TWIMS measurements show an average 0.62% absolute bias relative to DTIMS measurements, giving high confidence that the same conformers as in DTIMS experiments are being observed.

The percentage of open conformer is calculated to be 83% under the conditions specified in Materials and Methods, similar to the percentage in DTIMS experiments, demonstrating that ion heating is not significant under typical mobility settings. Previous work using leucine enkephalin as a thermometer ion has shown that bias voltage and traveling wave parameters, such as wave height, can contribute to field heating;[28,29,33] therefore, the effect of these parameters on the abundance of the open conformer has been evaluated. Separately, bias voltage is varied from 20 to 32 V and wave height from 7 to 10 V; outside these ranges, ion transmission or mobility resolution is poor. For easier viewing, voltages are normalized to the initial voltage and plotted on the same axis versus the percent open conformer in Figure 4. A trend of

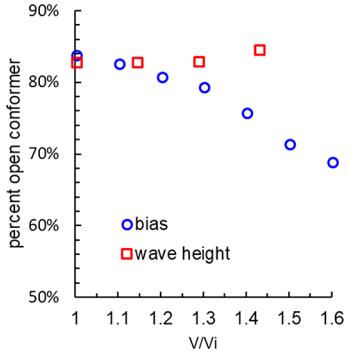

Figure 4. Percent open conformer of sodiated d_6-25OHD3 analyzed by TWIMS. Instrument voltages are normalized to the initial voltage for visualization. Wave height has no effect on percent open conformer, but bias voltage drives interconversion from open to closed.

decreasing percentage of open conformers from 84% to 69% is observed as the bias voltage is increased. The same trend is not true for wave height, where no interconversion is observed at any wave height. A slight increase in open conformers is observed at high wave height but is attributed to poorer resolution between the conformers. These results are consistent with previous studies by Merenbloom,[33] who finds

DOI: 10.1021/acs.analchem.8b05723
Anal. Chem. 2019, 91, 4092−4099

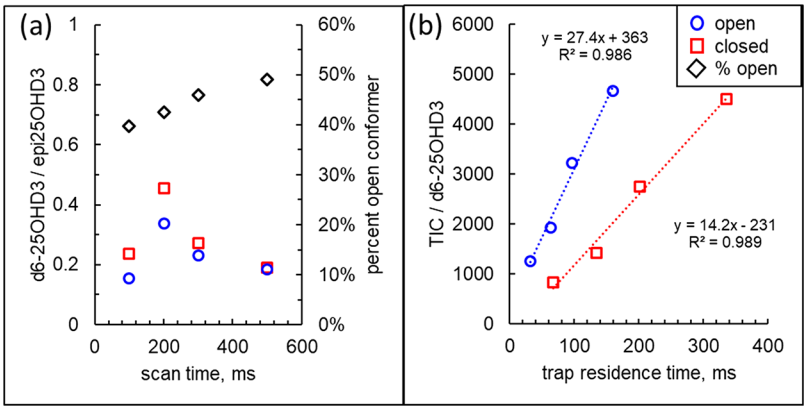

Figure 5. (a) Open and closed sodiated d_6-25OHD3 conformer abundance normalized to sodiated epi25OHD3 and percent open conformer at various scanning times. The percent of open conformer appears to increase with trapping time; however, when it is normalized to the epimer abundance, no conversion from closed to open is observed. (b) Fitting the ion concentrations to second-order kinetics shows that the open to closed conversion occurs more rapidly than the closed to eliminated reaction.

that bias voltage has the greatest effect on dissociation of leucine enkephalin, whereas the wave height has little effect. Even at high bias voltage, the open conformer remains the dominant species, suggesting that the time scale of the high-energy motion is likely too short for substantial interconversion.

The identity of the sodiated d_6-25OHD3 conformers are confirmed by CCS measurements to closely match those observed with traditional DTIMS, giving high confidence that the same conformers are being measured. Also, the ratio of open to closed conformers is closely aligned with that for DTIMS, detecting primarily the open conformer which is required for quantitation. Peak resolution between the open and closed conformers is poorer; the closed conformer is not completely resolved from the open conformer (R_s = 1.0). Newer TWIMS instruments claim an R_p value of 30,[37] substantially higher than the average R_p value of 15 measured here, which is typical for the previous generation technology;[37] however, even using the previous generation instrument, near-baseline resolution is achieved, and the open conformer survives throughout the IMS separation, suggesting that traveling wave ion mobility remains a potential platform for separation of sodiated 25OHD conformers.

Trapped IMS. Over a 0.12 V/ms scan rate, trapped IMS resolves two peaks for sodiated d_6-25OHD3 at 209.2 and 237.1 Å^2 and as well as two partially resolved IMS peaks at 208.6 and 211.2 Å^2 for the sodiated epi25OHD3. Using the reference CCS values (Table 1) to assign the identity of the peaks detected by TIMS, the lower CCS peaks correspond to the reference CCS of the closed conformer, while the higher CCS peaks correspond to the reference CCS of the open conformer with an average absolute bias for the four peaks of 0.49% to the reference values, showing good agreement. An average resolving power of R_p = 115 permits the resolution of two mobility peaks for sodiated epi25OHD3 by TIMS, in comparison to DTIMS and TWIMS, where only one peak is observed (Figure 2a–d). The second peak is likely present in the other ion mobility instruments, but the resolving power is too low to clearly resolve. Fitting the ion mobility spectrum with Gaussian peaks can deconvolute the additional peak. In Figure S2, two peaks were deconvoluted from the AP-DTIMS spectrum (ΔCCS = 1.1 Å^2), in comparison to the two TIMS peaks (ΔCCS = 2.5 Å^2). However, the structure of the additional conformer is currently unknown and will be the subject of future work. Although slower scan rates provide better resolving power,[38] they limit sampling across a chromatographic peak since fewer IMS scans can be completed. During an LC experiment, the duty cycle time should be minimized to improve the detail of the chromatographic peak, and in this case, a scan rate of 0.12 V/ms is able to resolve the open and closed conformers (R_s = 8.4) and still maintain a favorable duty cycle for coupling with liquid chromatography. Adams et al. used a 1.55 V/ms scan rate for LC-TIMS-MS quantitation of opioid isomers with ∼10% duty cycle in a single-stage TIMS analyzer similar to that utilized in this work,[39] which could be further enhanced to near 100% duty cycle using parallel accumulation.[40]

In contrast to DTIMS, which utilizes a dc electric field gradient within the drift tube, TIMS confines the ions within a stacked-ring electrode trap that uses rf fields to radially confine ions. Longer scan times increase the time scale that the ions reside within the trap, increasing their exposure to rf fields, which could convert the open to the closed conformer. As scan time increases, the percentage of the open conformer appears to increase from 40% at 100 ms to 48% at 500 ms scan time (Figure 5a), but this interpretation does not account for the differences in residence time of each ion within the trap. Using percent open conformer to track ion heating simplifies the interpretation of interconversion by assuming that the reaction proceeds from the open to closed conformer but ignores further elimination of the closed conformer by either collision with the electrode or loss of sodium ion. Normalizing the abundance of each conformer to that of sodiated epi25OHD3, which only forms the closed conformer, accounts for the elimination of the closed conformer by assuming that the epimer behaves similarly to the closed sodiated d_6-25OHD3. When interconversion occurs, the normalized closed and open values diverge in a mirror image;[16] however, during TIMS analysis, as the scan time increases, the conformers do not diverge but track closely (Figure 5a); this behavior can be attributed to the difference in trap residence time. In TWIMS and DTIMS, both conformers leave the drift tube within 4 ms of each other, representing a small fraction of the IMS separation, but during TIMS, the residence time of the closed conformer is twice that of the open conformer (TIMS elutes lower mobility ions first). Figure 5b shows the inverse of the ion concentration versus trap residence time during scanning (not counting the trap fill and separation time), which can be

DOI: 10.1021/acs.analchem.8b05723
Anal. Chem. 2019, 91, 4092–4099

fitted to a linear regression and reaction rate parameters extracted using the second-order kinetic rate law. The concentration of each conformer can be calculated as the abundance over the total ion counts (all ions at all m/z). The rate constant of the open conformer fit, representing the rate constant of the open to closed reaction, is greater than that of the closed conformer rate constant, representing the closed to eliminated reaction, consistent with the conclusion that IE increase first drives conversion from open to closed and then elimination at sufficiently high energy or time. The longer an ion resides in the rf trap, the greater the opportunity for undergoing conversion and elimination.

When it is coupled with LC, the scan rate should be optimized to provide sufficient detail on the chromatographic time scale by maximizing sampling across the LC peak. At 0.12 V/ms scan rate, the open conformer is still measured with sufficient abundance and resolution to allow further reductions of scan rate during LC/IM-MS method development. The high resolving power observed here (R_p = 115) is possible due to the limited mobility window being scanned, which would be the case in a targeted application. For untargeted acquisitions, a larger mobility window is required and a faster scan rate to ensure adequate sampling.

High-Field Asymmetric IMS. While all four low-field IMS instruments were able to resolve two peaks for sodiated d_6-25OHD3, FAIMS only detected one peak at CF = 1.8 Td and DF = 240 Td. Unlike DTIMS and TWIMS, two peaks were detected for sodiated epi25OHD3, a broad peak at CF = 2 Td and a narrow peak at CF = 3.1 Td (Figure 2e). Because FAIMS does not separate on the basis of CCS differences, it is not clear which conformers these peaks represent. In a patent, Kobold demonstrated epimer separation of the sodiated adducts using FAIMS.[41] Similar to our results, overlap is seen between an additional broad sodiated epi25OHD3 peak and the 25OHD3 peak; however, the interfering species was not identified. Using other alkali cations, such as rubidium, reduced the presence of the interfering species, though not completely eliminating it. To better understand the reversed separation (one sodiated d_6-25OHD3 peak and two sodiated epi25OHD3 peaks), the d_6-25OHD3 solution is infused with the BP salts at progressively higher dispersion fields to track internal energy changes with the evolution of the sodiated epi25OHD3 peaks.

Survival yield of the BP ions during FAIMS separation is measured between DF = 0 Td and DF = 280 Td and is plotted in Figure S3. Optimum separation of the sodiated epi25OHD3 peaks is achieved at 240 Td (Figure 2e), where survival yields of 72%, 78%, and 96% are measured for *p*-chloro-, *p*-(trifluoromethyl)-, and *p*-nitrobenzylpyridinium, respectively (Figure S3). From the lowest (DF = 0 Td) to the highest dispersion field (DF = 280 Td), survival yields remain effectively constant, suggesting that there is no significant change in the internal energy and that the additional FAIMS peak observed in the epimer spectrum is likely a conformer unresolved at lower dispersion fields rather than a product of interconversion driven by high dispersion fields. Scanning the compensation field from CF = −14 to 14 Td does not reveal an additional peak for sodiated d_6-25OHD3 or epi25OHD3 that would correspond to the second conformer observed in low-field IMS. While work by others finds internal energy increases with dispersion field, these experiments use planar FAIMS cells[42−44] with a channel length of 13 mm[43] and ion residence times of around 3 ms, in contrast to the chip-based FAIMS cell used in this experiment, which has a 700 μm channel length and ion residence times below 40 μs.[45] While ion activation could occur during the FAIMS separation, ions are readily cooled after passing through the cell in the atmospheric-pressure region before fragmentation or interconversion can occur. During low-field IMS experiments, sodiated epi25OHD3 is not shown to form the open conformer under any conditions due to the high energy difference between the conformers;[24] however, trapped IMS experiments reveal the presence of two overlapping conformers for sodiated epi25OHD3 (Figure 2d) that are not resolved by other low-field methods. At longer scan times and higher resolution, the conformers become more clearly resolved, although the ratio of the two peaks does not change. It is possible that the two sodiated epi25OHD3 peaks detected by FAIMS correspond to the two peaks detected by TIMS and can be confirmed with future work.

CONCLUSIONS

This study utilizes a single small ion, sodiated 25OHD3, to understand the separating power and internal energy sources in five ion mobility instruments encompassing a comprehensive profile of the commercial ion mobility spectrometry technologies. The four low-field IMS implementations, AP-DTIMS, LP-DTIMS, TWIMS, and TIMS, successfully separate the sodiated d_6-25OHD3 conformers; only FAIMS is unable to separate the sodiated conformers. For each instrument, relevant instrument parameters are identified as sources of internal energy which drive conversion of the fragile open conformer to the closed conformer; in this fashion, sodiated 25OHD3 acts as a thermometer ion for comparing ion mobility processes that is more sensitive and readily available than traditional thermometer ions. Future work should include detailed calculations modeling the energetics of the conversion of open to closed conformer for sodiated 25OHD3 to allow quantitative evaluations of internal energy changes.

Our primary interest is to use IMS with LC/MS to improve the quantitation of 25OHD, which requires the separation of the sodiated 25OHD conformers. While this study identifies which instruments separate the two conformers, it does not investigate the common figures of merit required for validation of a quantitative method, including limits of detection, linear range, or sensitivity. With greater options for instrument choices, laboratories interested in quantitation of 25OHD using this approach can better tailor their instrument selection to the other needs of the laboratory whether existing IMS instrumentation is used or new instruments are acquired.

ASSOCIATED CONTENT

Supporting Information

The Supporting Information is available free of charge on the ACS Publications website at DOI: 10.1021/acs.analchem.8b05723.

Instrument parameters, collision cross section calibration methods, compound structures, resolving power and resolution, and additional figures as described in the text (PDF)

AUTHOR INFORMATION

Corresponding Author

*Phone: 352-392-0557; Fax: 352-392-4651; Email: ryost@chem.ufl.edu.

DOI: 10.1021/acs.analchem.8b05723
Anal. Chem. 2019, 91, 4092−4099

ORCID
Francisco Fernandez-Lima: 0000-0002-1283-4390
Richard A. Yost: 0000-0002-1293-5669

Notes

The authors declare no competing financial interest.

■ ACKNOWLEDGMENTS

The authors would like to thank Agilent, Wellspring Clinical Laboratory, and National Institute of Health grant #U24DK097209 for funding.

■ REFERENCES

(1) Bikle, D. D. *Chem. Biol.* **2014**, *21* (3), 319−329.
(2) Liu, X.; Baylin, A.; Levy, P. D. *Br. J. Nutr.* **2018**, *119* (08), 928−936.
(3) Hyppönen, E.; Power, C. *Am. J. Clin. Nutr.* **2007**, *85* (3), 860−868.
(4) Haussler, M. R.; Jurutka, P. W.; Mizwicki, M.; Norman, A. W. *Best Pract. Res. Clin. Endocrinol. Metab.* **2011**, *25* (4), 543−559.
(5) Holick, M. F. *Ann. Epidemiol.* **2009**, *19* (2), 73−78.
(6) Wagner, D.; Hanwell, H. E.; Schnabl, K.; Yazdanpanah, M.; Kimball, S.; Fu, L.; Sidhom, G.; Rousseau, D.; Cole, D. E. C.; Vieth, R. *J. Steroid Biochem. Mol. Biol.* **2011**, *126* (3−5), 72−77.
(7) Powe, C. E.; Evans, M. K.; Wenger, J.; Zonderman, A. B.; Berg, A. H.; Nalls, M.; Tamez, H.; Zhang, D.; Bhan, I.; Karumanchi, S. A.; et al. *N. Engl. J. Med.* **2013**, *369* (21), 1991−2000.
(8) El-Khoury, J. M.; Reineks, E. Z.; Wang, S. *Clin. Biochem.* **2011**, *44* (1), 66−76.
(9) van den Ouweland, J. M. W. *TrAC, Trends Anal. Chem.* **2016**, *84*, 117−130.
(10) Bailey, D.; Veljkovic, K.; Yazdanpanah, M.; Adeli, K. *Clin. Biochem.* **2013**, *46* (3), 190−196.
(11) Kamao, M.; Tatematsu, S.; Sawada, N.; Sakaki, T.; Hatakeyama, S.; Kubodera, N.; Okano, T. *J. Steroid Biochem. Mol. Biol.* **2004**, *89*−*90*, 39−42.
(12) Singh, R. J.; Taylor, R. L.; Reddy, G. S.; Grebe, S. K. G. *J. Clin. Endocrinol. Metab.* **2006**, *91* (8), 3055−3061.
(13) Stokes, C. S.; Lammert, F.; Volmer, D. A. *Anticancer Res.* **2018**, *38* (2), 1137−1144.
(14) Strathmann, F. G.; Sadilkova, K.; Laha, T. J.; LeSourd, S. E.; Bornhorst, J. A.; Hoofnagle, A. N.; Jack, R. *Clin. Chim. Acta* **2012**, *413* (1−2), 203−206.
(15) Couchman, L.; Benton, C. M.; Moniz, C. F. *Clin. Chim. Acta* **2012**, *413* (15−16), 1239−1243.
(16) Oranzi, N. R.; Polfer, N. C.; Lei, J.; Yost, R. A. *Anal. Chem.* **2018**, *90* (22), 13549−13556.
(17) Hoaglund, C. S.; Valentine, S. J.; Sporleder, C. R.; Reilly, J. P.; Clemmer, D. E. *Anal. Chem.* **1998**, *70* (11), 2236−2242.
(18) May, J. C.; Goodwin, C. R.; Lareau, N. M.; Leaptrot, K. L.; Morris, C. B.; Kurulugama, R. T.; Mordehai, A.; Klein, C.; Barry, W.; Darland, E.; et al. *Anal. Chem.* **2014**, *86* (4), 2107−2116.
(19) Lapthorn, C.; Pullen, F.; Chowdhry, B. Z. *Mass Spectrom. Rev.* **2013**, *32* (1), 43−71.
(20) Mason, E. A.; Schamp, H. W. *Ann. Phys.* **1958**, *4*, 233−270.
(21) Pringle, S. D.; Giles, K.; Wildgoose, J. L.; Williams, J. P.; Slade, S. E.; Thalassinos, K.; Bateman, R. H.; Bowers, M. T.; Scrivens, J. H. *Int. J. Mass Spectrom.* **2007**, *261* (1), 1−12.
(22) Michelmann, K.; Silveira, J. A.; Ridgeway, M. E.; Park, M. A. *J. Am. Soc. Mass Spectrom.* **2015**, *26* (1), 14−24.
(23) Shvartsburg, A. A.; Tang, K.; Smith, R. D.; Holden, M.; Rush, M.; Thompson, A.; Toutoungi, D. *Anal. Chem.* **2009**, *81* (19), 8048−8053.
(24) Chouinard, C. D.; Cruzeiro, V. W. D.; Beekman, C. R.; Roitberg, A. E.; Yost, R. A. *J. Am. Soc. Mass Spectrom.* **2017**, *28* (8), 1497−1505.
(25) Gabelica, V.; De Pauw, E. *Mass Spectrom. Rev.* **2005**, *24* (4), 566−587.
(26) Naban-Maillet, J.; Lesage, D.; Bossée, A.; Gimbert, Y.; Sztáray, J.; Vékey, K.; Tabet, J. C. *J. Mass Spectrom.* **2005**, *40* (1), 1−8.
(27) Morsa, D.; Gabelica, V.; Rosu, F.; Oomens, J.; De Pauw, E. *J. Phys. Chem. Lett.* **2014**, *5* (21), 3787−3791.
(28) Morsa, D.; Gabelica, V.; De Pauw, E. *Anal. Chem.* **2011**, *83* (14), 5775−5782.
(29) Morsa, D.; Gabelica, V.; De Pauw, E. *J. Am. Soc. Mass Spectrom.* **2014**, *25* (8), 1384−1393.
(30) Carpenter, J. E.; McNary, C. P.; Furin, A.; Sweeney, A. F.; Armentrout, P. B. *J. Am. Soc. Mass Spectrom.* **2017**, *28* (9), 1876−1888.
(31) Kuki, Á.; Shemirani, G.; Nagy, L.; Antal, B.; Zsuga, M.; Kéki, S. *J. Am. Soc. Mass Spectrom.* **2013**, *24* (7), 1064−1071.
(32) Schnier, P. D.; Price, W. D.; Strittmatter, E. F.; Williams, E. R. *J. Am. Soc. Mass Spectrom.* **1997**, *8* (97), 771−780.
(33) Merenbloom, S. I.; Flick, T. G.; Williams, E. R. *J. Am. Soc. Mass Spectrom.* **2012**, *23* (3), 553−562.
(34) Badman, E. R.; Hoaglund-Hyzer, C. S.; Clemmer, D. E. *Anal. Chem.* **2001**, *73* (24), 6000−6007.
(35) D'Atri, V.; Causon, T.; Hernandez-Alba, O.; Mutabazi, A.; Veuthey, J.-L.; Cianferani, S.; Guillarme, D. *J. Sep. Sci.* **2018**, *41* (1), 20−67.
(36) Stow, S. M.; Causon, T. J.; Zheng, X.; Kurulugama, R. T.; Mairinger, T.; May, J. C.; Rennie, E. E.; Baker, E. S.; Smith, R. D.; McLean, J. A.; et al. *Anal. Chem.* **2017**, *89* (17), 9048−9055.
(37) Zhong, Y.; Hyung, S. J.; Ruotolo, B. T. *Analyst* **2011**, *136* (17), 3534−3541.
(38) Fernandez-Lima, F.; Kaplan, D. A.; Suetering, J.; Park, M. A. *Int. J. Ion Mobility Spectrom.* **2011**, *14* (2), 93−98.
(39) Adams, K. J.; Ramirez, C. E.; Smith, N. F.; Muñoz-Muñoz, A. C.; Andrade, L.; Fernandez-Lima, F. *Talanta* **2018**, *183*, 177−183.
(40) Silveira, J. A.; Ridgeway, M. E.; Laukien, F. H.; Mann, M.; Park, M. A. *Int. J. Mass Spectrom.* **2017**, *413*, 168−175.
(41) Kobold, U.; Thiele, R.; Weiss, N.; Brown, L. METHOD AND DEVICE FOR SEPARATING METABOLITES OR STEREOISOMERS BY ION MOBILITY SPECTROMETRY. WO/2015/185487 A1, 2005.
(42) Santiago, B. G.; Campbell, M. T.; Glish, G. L. *J. Am. Soc. Mass Spectrom.* **2017**, *28* (10), 2160−2169.
(43) An, X.; Eiceman, G. A.; Rodriguez, J. E.; Stone, J. A. *Int. J. Mass Spectrom.* **2011**, *303* (2−3), 181−190.
(44) Levin, D. S.; Vouros, P.; Miller, R. A.; Nazarov, E. G.; Morris, J. C. *Anal. Chem.* **2006**, *78* (1), 96−106.
(45) Wilks, A.; Hart, M.; Koehl, A.; Somerville, J.; Boyle, B.; Ruiz-alonso, D. *Int. J. Ion Mobility Spectrom.* **2012**, *15*, 199−222.

DOI: 10.1021/acs.analchem.8b05723
Anal. Chem. 2019, 91, 4092−4099